Electrochemical Corrosion Inhibition Process, Adsorption Mechanism and Mechanical Effect of *Newbouldia laevis* Leaf Extract on Aluminum Alloy in Acidic Environment

Nwosu Okechukwu Francis[1,2*], Israel O. Owate[2] and Eziaku Osarolube[2]

[1]*Department of Physics and Electronics, Abia State Polytechnics, Aba, Abia State, Nigeria.*
[2]*Department of Physics, University of Port Harcourt, Choba, Rivers State, Nigeria.*

Authors' contributions

This work was carried out in collaboration between all authors. All authors read and approved the final manuscript.

Original Research Article

ABSTRACT

Aims: This research is aimed at using advanced corrosion identification and corrosion inhibition technique to investigate the corrosion inhibition mechanism of Al Alloy (AA5052) in 1.0 M HCl solution using *Newboudia laevis* leaf extract.
Place and Duration of Study: The research was carried out at Material Science Laboratory Group, Physics/Electronic Department, Abia State Polytechnic, Aba Abia State.
Methodology: Extraction of the green leaf was done with reflux apparatus under constant temperature. The 100% inhibitor solvent was diluted to the various inhibitor concentrations. Gravimetric technique and electrochemical impedance spectroscopy (EIS) were employed to study the corrosion and corrosion inhibitory behavior of the metal in the various environments. Scanning Electron Microscope and OPTICAL emission microscopy were used to investigate the surface structure of the corroded and inhibited metal alloy. The influence of the leaf extract on the mechanical hardness of the Al alloy AA5052 was tested using Vickers indentation hardness test.

Corresponding author: E-mail: nwosufranciso@yahoo.com;

Results: The presence of the *Newbouldia leavis* leaf extract significantly reduced the weight loss and also decreased the rate of chemical attack on the AA5052 alloy. The inhibition efficiency of the inhibitor increases with increase in concentration but decreased with increase in temperature. The introduction of the leaf extract alters the electrochemical behaviours of the metal in the acidic environment. The inhibitor mechanism was found to be through adsorption on the metal surface according to Langmuir adsorption isotherm. The Gibb's free energy confirms that the inhibition of the leaf to corrosion attacks is spontaneous. The calculated activation energy, heat of adsorption, enthalpy and the entropy implications of the leaf extract were appraised. The surface morphology of the metal was studied to ascertain the level of redemption offered by the green inhibitor molecules to the material degradation. Vickers hardness test revealed that the presence of the inhibitor improved the mechanical hardness of the corroded Al alloy.
Conclusion: The acidic corrosion of AA5052 has been studied. The study shows that *Newboudia laevis* extract can be used to combat the corrosion attacks on AA5052 alloy.

1. INTRODUCTION

Aluminum and its alloy is one of the most used materials. Aluminum has low density, high ductility, high thermal and electrical conductivity, good corrosion resistance, attractive appearance, and it is nontoxic. Despite its cost, this remarkable combination of qualities makes it a preferred choice for many critical applications in aerospace, automobiles, food handling, building, heat exchange, and electrical transmission [1,2].

Despite the corrosion resistance nature of Aluminum due to its ability to form thin film called oxide which serves as a protective surface film [2]; Al still reserve a very distinct position in industrial uses such as reaction vessels, pipes, machinery and chemical batteries [3]. However, in service, Al falls short in its properties as a result of corrosion attack.

Corrosion is the disintegration of a material or its properties by reaction when interacting with its surrounding environment [4]. Nwosu and Osarolube [5] noted that corrosion phenomena, control and prevention are unavoidable major scientific issues that must be addressed daily as far as there are increasing needs of metallic materials in all facets of technological development. There are several methods to protect aluminum and its alloys, among which the anodising process, coatings, paints, organic coatings, and corrosion inhibitors are found to be the most effective. The safety and environmental issue of corrosion inhibitors arisen in industries has always been a global concern. Chromates for example are used in the pretreatments of aluminum alloys and they are found to be both toxic and carcinogenic [6]. This demerit of synthesized inhibitors gave birth to organic inhibitor. Okafor et al. [7] and Umoren et al. [8] noted that organic inhibitors are benign, eco-friendly, readily available, cheap, and their extracts are rich sources of molecules which have appreciably high inhibition efficiency and hence termed as "Green Inhibitors".

Researchers have made tremendous contributions in limiting the dangers of corrosion and corrosion products. This research is aimed contributing to the growing trend on the corrosion inhibition of Al alloy in acidic environment.

2. MATERIALS AND METHODS

2.1 Materials Preparation

Nowbouldia laevis leaf were collected from Uzuakoli forest (5°38′0″ North, 7°34′0″ East) in Abia State Nigeria, washed, air dried away from direct sunlight, and then ground to powder (the solute). The extraction is then carried out under reflux (ration of 1:10, solute/solvent) in accordance to the method used by Nwosu et al. [9], Oguzie et al. [10] at constant temperature 65°C for 3 hours. The solvent used was the corrosive environment. The solution was cooled under atmospheric pressure. The filtrate measured. Then the various inhibitive environments prepared (diluted) in the range 0.1 - 0.5 g/L.

The aluminum alloy AA5052 used for the research was machine cut in coupons of 20 mm x 20 mm x 10 mm with 2 mm hole for suspension in the test solution. The aluminum alloy consists the following 98.8% Al-PURE. The coupon were washed thoroughly with distilled water

and degreased with ethanol and acetone, air dried before being immersed in the acid solution.

The test solution, the corrosive environment was prepared and some part used for the extraction of the plant produce [11]. The 100% inhibitor (the filtrate) was further diluted to various concentrations.

2.2 Gravimetric Technique

The gravimetric technique was employed to observe the general corrosion behavior and the inhibitive process. The prepared weighed coupons were initially weighed with an FA2104A analytical electronic digital weighing balance: sensitivity of 0.0001. The prepared coupons were subjected to investigation by suspending them fully immersed in a 300 ml beaker containing 250 ml various concentrations of the inhibitor. Water bath was used to vary the temperatures (30°C, 45°C and 60°C) of the corrosion study. After the exposure period, the coupons were retrieved from the environment (test solutions), washed in a double distilled water, rinsed in acetone and air dried before reweighing. The weight of the respective coupon and time was recorded as the initial weight minus the final weight. Triplicate investigations were carried out and the average recorded for reproducibility.

2.3 Electrochemical Impedance Spectroscopy (Eis) Technique

The electrochemical impedance spectroscopy (EIS), a complimentary technique provides information on the capacitive behavior of the system and monitors the electron transfer rate of reaction.

Li et al. [11], Iroha et al. [12] and Nwosu et al. [13] had earlier described the EIS procedure of the electrochemical advanced technique employed. Electrochemical tests were conducted using a PAR-2273 Advanced Electrochemical System Work station using standard three electrode electrochemical cell. The working electrode is aluminum AA5052. A saturated calomel electrode (SCE) was used as the reference electrode, while a graphite rod was used as the counter electrode. The coupon AA5052 which served as the working electrode was fixed in epoxy resin with a surface area of 1.0 cm^2 exposed to the test solution.

Electrochemical measurements were carried out in aerated and unstirred solutions at the end of 3600 s of immersion, which allowed the Open Circuit Potential (OCP) values to attain steady state. Temperature was fixed at 30±1°C. The polarization resistance was monitored. Triplicate experimental were carried out and the average value recorded.

2.4 Mechanical Hardness Indentation Test

The coupons/samples subjected to mechanical hardness testing were not surface tempered. The Hardness mechanical tests were performed on the AA5052 coupons with a load of 10 N. The Vickers microindentation tests were performed at different locations on the metal surface as reported earlier by Nwosu et al. [13], Nwosu et al. [14]. Five different indentations were made on the coupons and the average value reported.

3. RESULTS AND DISCUSSION

3.1 Weight Loss and Corrosion Rate

The general corrosion parameters; weight loss and the corrosion rate behavior of AA5052 Al alloy. Fig. 1 showed the weight loss (in grams) variation of the AA5052 with exposure time (in hours). The Weight losses were found to increase linearly with increasing exposure time. The introduction of *N. laevis* in the enabling environment reduced the material degradations at every interval of inspection.

The Corrosion rate, CR (in mil per yr) was calculated from the values obtained from weight loss using equation 1 [15] shown in Fig. 2 showed that there were great reduction in corrosion rate in the presence of the inhibitor. The trend in corrosion rate apparently becomes linear at later exposed period.

$$CR = \frac{87.6 \ \Delta W}{A \rho t} \tag{1}$$

ΔW is the weight loss, A is the surface area exposed to corrosion study (in cm^2), ρ is the density of the metal (in g/cm^3), t is the immersion period (in hours). These reductions are accordance to the definition of inhibitor offered by Sastri [16] that corrosion inhibitor is a chemical substance that upon addition to a corrosive environment, results in reduction of corrosion rate to an acceptable level.
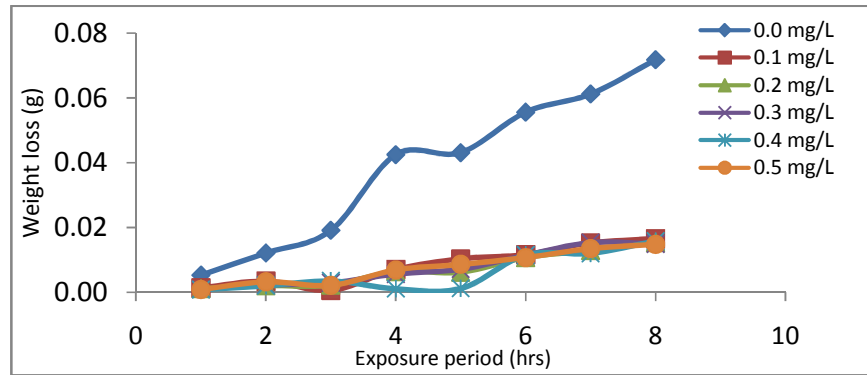
Fig. 1. Weight loss variation with exposure period of AA5052 in 1.0 M HCl in the presence of *Newbouldia leavis* extract
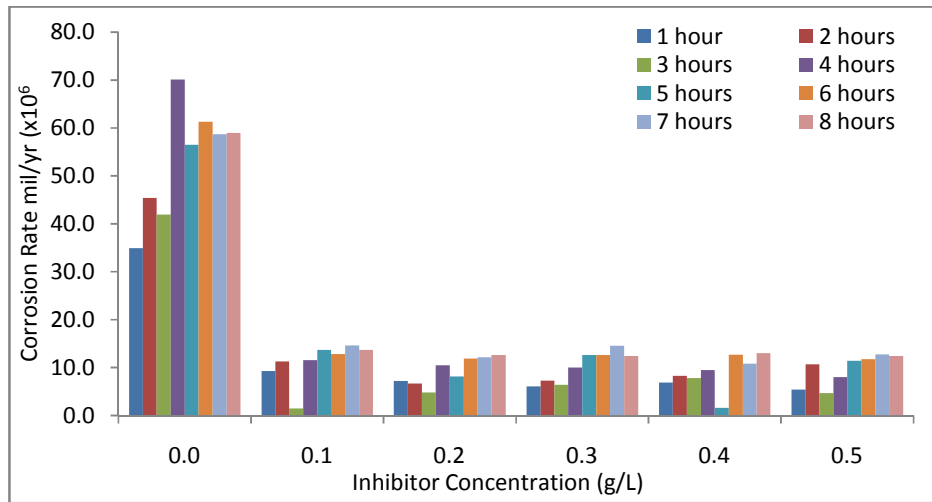

Fig. 2. Corrosion rate against inhibitor concentration of AA5052 in 1.0 M HCl in the presence of *Newbouldia leavis* extract
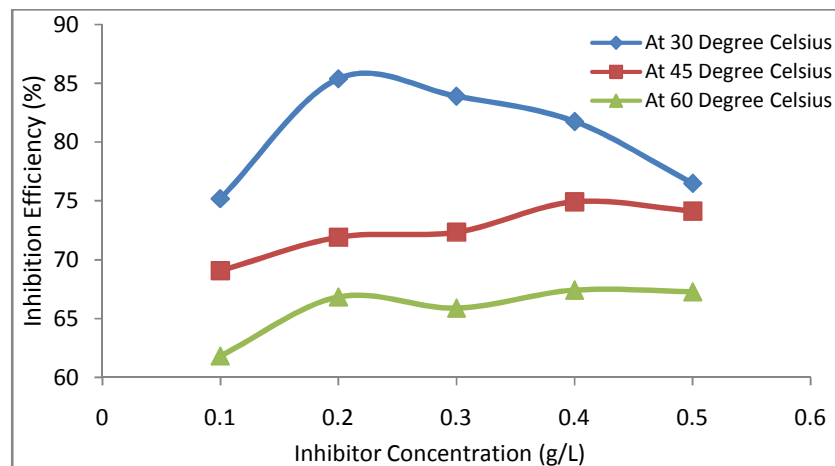

Fig. 3. Inhibition efficiency of *Newbouldia laevis* as a function of inhibitor

3.2 Inhibition Efficiency

Generally, corrosion inhibitor could be calculated from any observable parameters from corrosion studies. The corrosion inhibitor is rated in terms of inhibition efficiency %*IE* and is defined as (equation 2) [16,17].

$$\%IE = \left(1 - \frac{CR_{inh}}{CR_{free}}\right) \times 100 \qquad (2)$$

Where CR is the corrosion rate and the subscript inh and free refer, respectively to the presence and absence of the inhibitor. Fig. 3 showed that the inhibition efficiency increases with inhibitor concentration but decreases with temperature. One of the possible ways the inhibitor causes the increase with concentration is either by the actions of altering corrosive environment into a noncorrosive or less corrosive environment through its interaction with the corrosive species or the corrosion inhibitor interacts with the surface and renders protection of the metal from corrosion [16]. However, the adsorption isotherm would help analyze if the inhibitor is environment modifier or adsorption inhibitor.

3.3 Electrochemical Imedapnce Spectros-copy (Eis) Results

The Electrochemical impedance spectroscopy (EIS) was performed to study the corrosion of AA5052 Al alloy in 1.0 M HCl solution in the inhibited system and the inhibitor-free system. In EIS, the sensing element is usually polarized by the application of an alternating potential, which in turn produced an alternating current response. Fig. 4 showed the Nyquist plot/spectrum which characterized by semicircle. The semicircle offers the understanding that the as inhibitor concentration increases, the semicircle in radius increases. The Nyquist plot is a complex plane of Cartesian corrdinates, where the abscissa is the real part (resistive terms) and the ordinate is the imaginary part (capacitive or inductive terms) [18]. This indicates that there is a strong inductive loop as the inhibitor concentration increases. The capacitive loop arise from the time constant of the electric double layer and charge-transfer resistance, and an inductive loop appeared at low frequency values due to the presence of the inhibitor [19]. It may also be attributed to adsorption of inhibitor on the electrode surface [20] which creates barrier to current flow or to charge-transfer. R_{ct} represent the charge transfer resistance. It measures the

electron transfer across the surface, which is inversely proportional to the corrosion rate [21]. The larger the diameter of the semicircle, the higher the resistance R_{ct} and hence the lower the corrosion rate [22].

The curve fitting and simulation of the Nyquist plots was carried out by using the R(RQ) equivalent model circuit of the form in Fig. 5. This was used to model the impedance results (which is represented by Z, measures the relationship between *ΔE* and *ΔI*) obtained for the inhibited and uninhibited AA5052 samples in 0.5 M HCl solutions, after fitting with Zsimpwin software. The R_s is the solution resistance, while the inductance L, and the charge-transfer resistance R_{ct} characterize the inhibitor process beneath the store charges.

The inhibition efficiency (%IE) was calculated from the values of R_{ct} using equation 3 [23,24].

$$\%IE = \left(1 - \frac{R_{ct}}{R_{ct}^{\ominus}}\right) \times 100 \qquad (3)$$

Where R_{ct} and CR^0_{ct} are the charge-transfer resistance for the inhibited and uninhibited systems, respectively. Table 1 showed that there were corresponding increase in the R_{ct}, R_s and L due to the presence of the green inhibitor. An optimal inhibition efficiency of 88% was recorded at the maximum considered inhibitor concentration of the leaf extract.
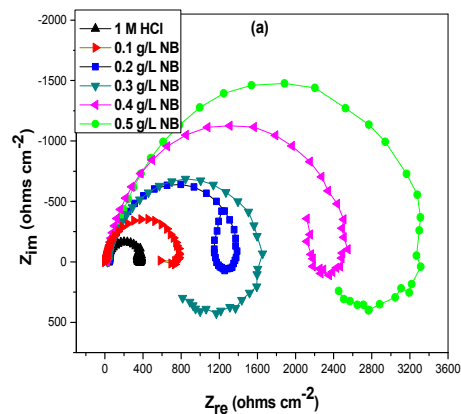
Fig. 4. Electrochemical impedance spectroscopy plots of Al in 1.0 M HCl solution in the absence and presence of different concentrations of *N. laevis*

3.4 Adsorption Isotherm Models and Theremodynamic Parameters

Adsorption is a surface phenomenon. The adsorption of inhibitors on the metal surface is governed by the residual charge on the metal and the chemical structure of the inhibitor. They are two possible adsorption types of an organic inhibitor: Physical or electrostatic and chemisorptions [17]. In a situation where it is suspected that the inhibition of metal corrosion occurred as a result of the adsorption of molecules of plant extract on to the metal surface, it is pertinent to investigate the possible adsorption model by testing the experimental data obtained with several adsorption isotherms such as Langmuir, Temkin, Flory-Huggins, Frumkin etc [25].
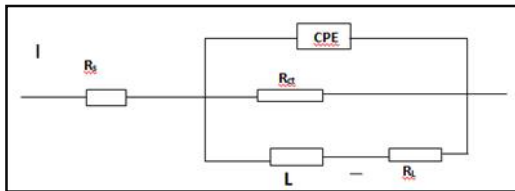

Fig. 5. The equivalent model circuit of the impedance spectra

Langmuir isotherm (equation 4) [24] provides the interpretation between the surface coverage, $(\Theta=\%IEx100)$, the adsorption equilibrium constant, K_{ads} and the inhibitor concentration, C. The plot of C/Θ vs C (Fig. 5) showed that the plot gives a straight line curve of slope, S, unity which confirms that the adsorption of *N. laevis* leaf extract on the metal's surface obeys Langmuir adsorption model with the correlation coefficient, R^2 close to unity. Table 2 shows the adsorption equilibrium constant and its corresponding Gibb's free energy of adsorption (equation 5) [25-27] at the varied temperature. The negative values of the free energy of adsorption at varied temperatures show that the adsorption of the inhibitor molecules on the metal surface was spontaneous and via physical adsorption process; decreases slightly with increase in temperature.

$$\frac{C}{\theta} = \frac{1}{K_{ads}} + C \qquad (4)$$

$$\Delta G_{ads} = -2.303RTLog(55.5K_{ads}) \qquad (5)$$

Where 55.5 (in $MolL^{-1}$) is molar concentration of water, R is the universal gas constant and T is the thermodynamic temperature.

Table 1. Electrochemical parameters for Al in uninhibited and inhibited 1.0 M HCl solution in the presence of *N. laevis* leaf extract

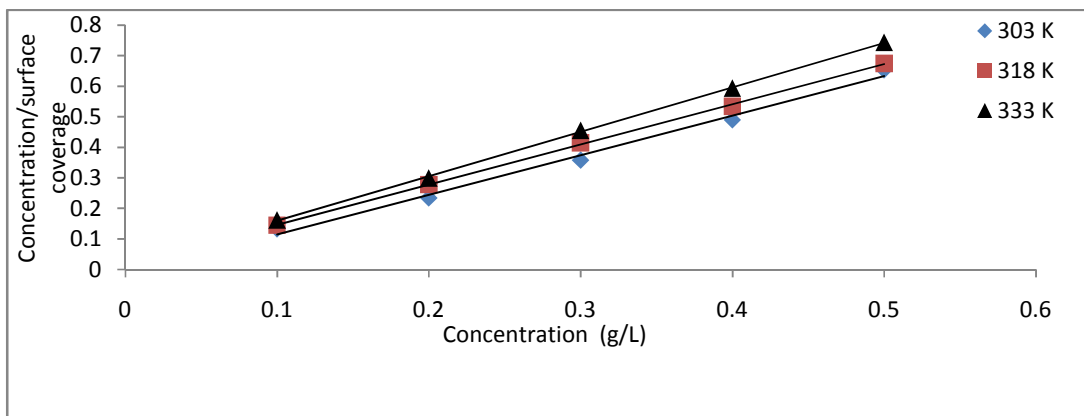| System *N. laevis* (g/L)	R_s (Ωcm^2)	R_{L1} (Ωcm^2)	R_{ct} (Ωcm^2)	L(H)	IE (%)
0.0	2.36	5.7	400	4.34	-
0.1	2.43	726	810	762	50.6
0.2	2.89	918	1300	1102	69.2
0.3	3.05	1214	1670	1432	76.1
0.4	3.25	2208	2508	2087	84.1
0.5	3.86	2875	3288	2983	87.8

Fig. 6. Lamgmuir isotherm of *N. laevis* adsorption on AA5052 aluminium alloy in 1.0 M HCL at varied temperatures

Table 2. Langmuir Isotherm parameters of *N. laevis* extract on AA5052 Al alloy in 1.0 M HCl solution

	Langmuir isotherm			
	S	**K_{ads}**	**R^2**	**G_{ads} ($KJ.mol^{-1}$)**
303	1.2967	64.935	0.9922	-20.6
318	1.3151	68.493	0.9995	-20.8
333	1.4567	74.074	0.9997	-21.0

The influence of temperature variation on the inhibitive system paved way to the study of the inhibition efficiency and the thermodynamic considerations. The thermodynamic parameters were evaluated using weight loss measurements in the temperature range 30-60°C. The activation energy of the corrosion with and inhibitor-free system were calculated by the Arrhenius equation (equation 6) [28, 29]. The equation 6 was rearranged to equation 7 which enabled us to calculate the apparent activation energy from the gravimetric measurements. The thermodynamic parameters were reported on Table 3. It showed that the apparent activation energy of the corrosion process was increased as the inhibitor concentration increases. This translates that the barrier needed for the corrosion process to start was raised by the presence of the *N. laevis*. The apparent activation energy also increased greatly with temperature increase. However, the heat of adsorption (equation 8) [29] of the inhibitor molecules decreases with increase in the inhibitor concentration. The negative values of Q_{ads} indicate that the process of inhibition is exothermic.

$$Log\ CR = \frac{-E_a}{2.303RT} + Log\ A \qquad (6)$$

$$Log\left(\frac{CR_2}{CR_1}\right) = \frac{E_a}{2.303R}\left[\frac{1}{T_1} - \frac{1}{T_2}\right] \qquad (7)$$

$$Q_{ads} = 2.303R\left[\log\left(\frac{\theta_2}{1-\theta_2}\right) - \log\left(\frac{\theta_1}{1-\theta_1}\right)\right] x \left[\frac{T_1 x T_2}{T_2 - T_1}\right] \qquad (8)$$

$$CR = \left(\frac{RT}{N_a h}\right) exp\left(\frac{\Delta S^*}{R}\right) exp\left(\frac{-\Delta H^*}{RT}\right) \qquad (9)$$

Where CR is the corrosion rate determined from the gravimetric measurements, E_a is the activation energy, R is the universal gas constant (8.3145J/mol-K), A is the Arrhenius frequenting factor. θ_1 and θ_2 are the surface coverage at temperature T_1 and T_2, respectively.

Table 3 shows that the calculated activation energy is related to the values obtained from the graph. This shows that both theoretical approach and graphical approach agreed to the nature of the inhibitor behaviours on the AA5052 Al alloy.

Some other activation parameters such as the enthalpy change of activation (ΔH^*) and entropy change of activation (ΔS^*) were obtained from the Eyring transition state equation (9) [30]. The Eyring plots (Fig. 8) gives linear plots from which the thermodynamic parameters such as the enthalpy and the entropy of activation were calculated from the slope and the intercept, respectively; and reported on Table 3. The positive values of ΔH^* in both inhibitive system and in the inhibitor-free system indicates an endothermic nature of the Al dissolution process [31]. Similar result was reported by Awe et al. [32]. The entropy, ΔS decreased with increase in inhibitor concentration expresses more ordered behavior of the inhibition efficiency. The decrease in magnitude of ΔS infers a more stable thin film layer of active molecules of the green leaf extract on the substrate surface as extract concentration increases [33].

3.5 Surface Morphology Studies

The surface screening or imaging was conducted using OPTICAL emission microscopy (Fig. 9) and scanning electron microscopy (SEM) (Fig. 10). It is imperative to investigate the damaging and protective effect of the corrosion environment and the corresponding inhibitive effect of *N. laevis* leaf extract on AA5052 in 1.0 M HCl. All the coupons were investigated without further surface treatment.

The SEM-imaging Fig. 9a reveals the nature of the AA5052 surface as received. The phases are seen to have an organized surface structure which could be attributed to the interface between the parent metal, Al and the other allowing element. But, Fig. 9b shows the surface of AA5052 retrieved from the inhibitor-free environment. This presents us with a surface with high density of porosity. This porosity is as a result of the chemical/electrochemical attack. The attack was found reduced when Fig. 9c is viewed. The Fig. 9c is the surface of AA5052 exposed to inhibited system. This establishes that the presence of *Newbouldia laevis* leaf extract in 1.0 M HCl solution reduced the nature of degradation of AA5052.

Table 3. Thermodynamic parameters for adsorption of *Newbouldia leavis* leaf extract on surface of Al alloy AA5052 at different concentrations

System	Graph data		Calculated data		ΔH^*	ΔS^*
(g/L)	E_a (KJ/mol)	A-Factor	E_a (KJ/mol)	Q_{ads} (KJ/mol)	(KJmol^{-1}K^{-1})	(Jmol^{-1}K^{-1})
0.00	61.06	1.48 x 10^{12}	61.13	-	25.37	-120.76
0.10	73.11	4.37 x 10^{13}	73.19	-33.51	30.60	-108.59
0.20	84.16	2.24 x 10^{15}	84.05	-56.87	35.40	-94.37
0.30	82.17	1.07 x 10^{15}	82.11	-52.97	34.53	-96.94
0.40	77.24	1.66 x 10^{14}	77.31	-41.22	32.39	-103.68
0.50	70.24	1.29 x 10^{13}	70.37	-24.52	29.35	-112.99
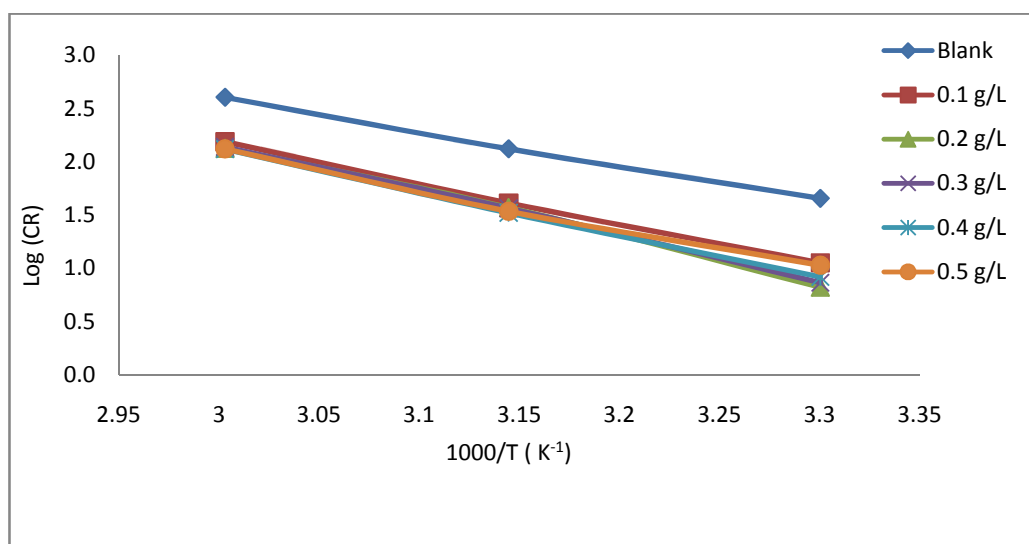
Fig. 7. Arrhenius plots to calculate the activation energy of corrosion of AA5052 in the presence and absence of *N. laevis* extract in 1.0 M HCl
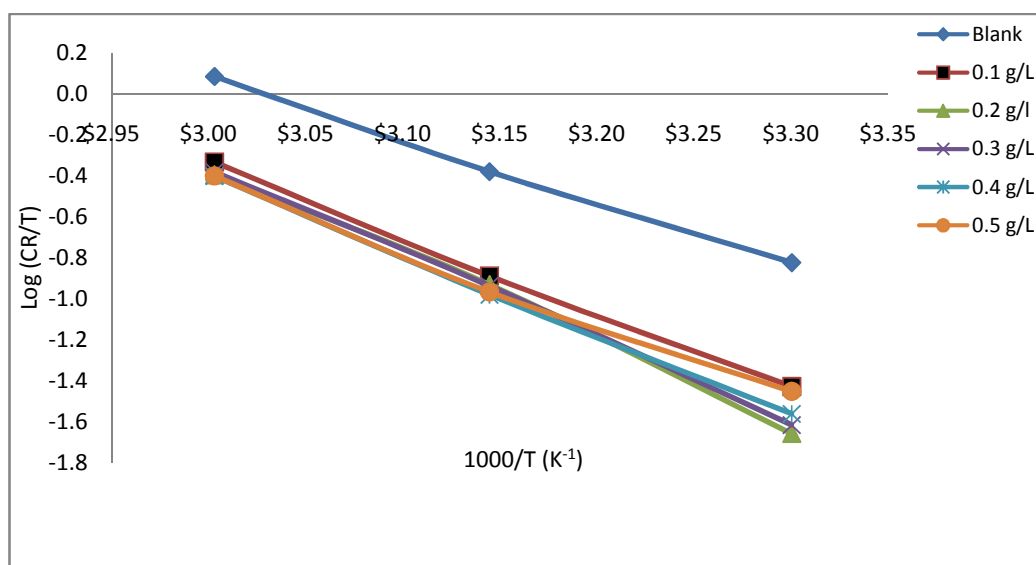
Fig. 8. Eyring plots of Log (CR/T) versus 1000/T for the corrosion of AA5052 the absence and presence of *N. laevis* extract in 1.0 M HCl solution
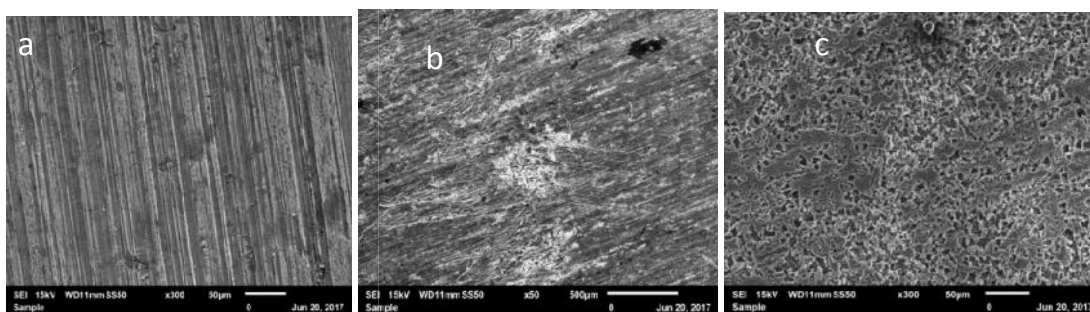
The OPTICAl micrograph of AA5052 (Fig. 10) supports the SEM-imaging results. Fig. 10a reviewed the normal surface of the coupon AA5052 containing the parent metals and the alloying metals. Fig. 10b reviewed much yellowish patches indicating that the parent metal was greatly attacked by the corrosive environment. However, Fig 10c shows the micrograph of the inhibited metal. It clearly reveals the nature of the thin film coverage of the *N. laevis* molecules on the surface of Al alloy. This thin film coverage is in accordance to adsorption findings: That the presence of the inhibitor caused a barrier between the metal surface and the enabling environment. Eye observation also recorded that during the immersion, the gas evolution was reduced in the case of the inhibited system.

3.6 Mechanical Hardness Test

The influence of the inhibitor on the mechanical hardness response of the metal was tested with Vickers Microindentation test shown in Fig. 11. The Vickers hardness value of the raw sample is greatest compared with other samples; indicating

100% hardness value of AA5052. The hardness of the metal reduced to 97.21% in the inhibitor-free environment. This value is low compared to that exposed in inhibited system (97.91%). The presence of the inhibitor actually improved the hardness value of the corroded AA5052 by 0.7%. This percentage increment of the hardness value is significant to combat corrosion failures.

It was suspected that the increment of the metal hardness could be attributed to the adsorption of the inhibitor molecules which extents discouraged the degrading of the metal. The presence of the inhibitor has been reported in this paper that it reduced the density of the porosity found in the metal after exposure. Porosity is a factor responsible for the expression of the microstructure of metal. Alteration in the microstructure of engineering materials affects the mechanical properties. The presence of the inhibitor molecule caused an improvement on the hardness value of the corroded AA5052 in acidic media. Aqida et al. [34] submitted that porosity is a defect formed by interfacial reactions, which causes a decrease in the mechanical properties.

Fig. 9. SEM imaging of AA5052 surface exposed to (a) RAW (as received), (b) 1.0 M HCl Inhibitor-free system and (c) Inhibitive system of N. laevis leaf extract
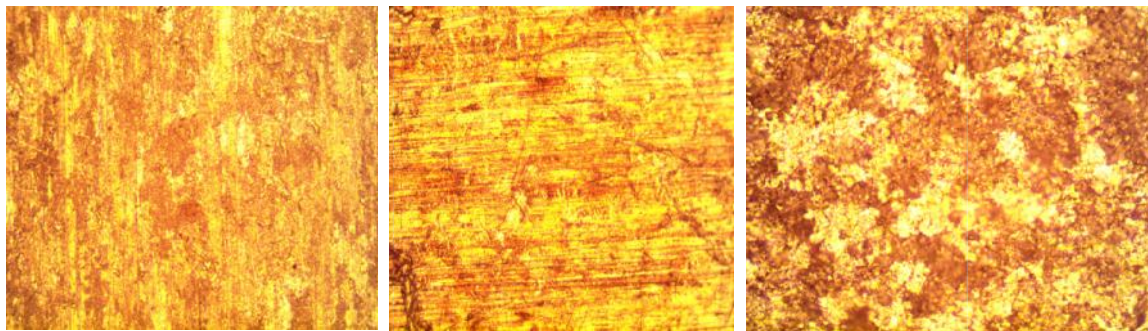
Fig. 10. Optical micrograph of AA5052 exposed to: (a) RAW (As received), (b) blank solution of 1.0 M HCl, (c) 1.0 M HCl solution containing N. laevis extract
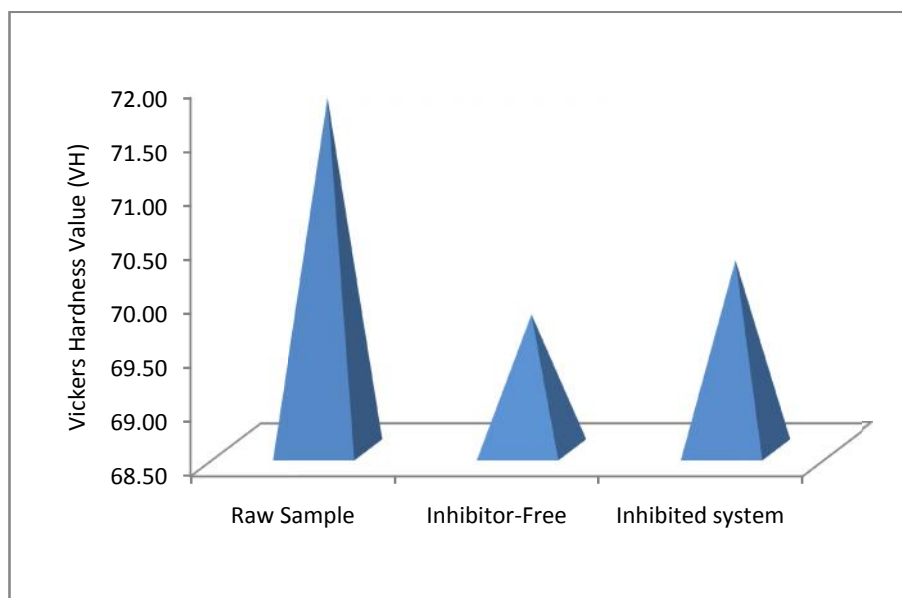
Fig. 11. Mechanical Vickers micro indentation value of AA5052 exposed to an acidic and inhibited environment

4. CONCLUSION

The corrosion inhibitor for AA5052 in acidic environment has been developed using *Newbouldia leavis* leaf extract. The efficiency of the leaf extracts increases with increase in concentration but, decreases with increase in temperature. The inhibition process was found to be through physical adsorption on the metal surface according to Langmuir adsorption model. The thermodynamic parameters studied showed that the adsorption process was spontaneous given the negative value of the free energy value (ΔG). The apparent corrosion activation reaction energies were increased due the presence of the inhibitor, while the entropy of the system reduced signifying a reduction in the rte of disorder of the reactant molecules. The studied further gave insight on the reduction of surface damage due to the presence of the inhibitor. Hardness value of the metal, AA5052 was improved after degradation as a result of the leaf extract.

COMPETING INTERESTS

Authors have declared that no competing interests exist.

REFERENCES

1. David T, James T. Corrosion science and technology, CRC. Series in Materials Science and Technology; 1998.

2. Patel AS, Pancha VA, Mudaliar GV, Shah NK. Impedance spectroscopic study of corrosion inhibition of Al-Pure by organic Schiff base in hydrochloric acid. Journal of Saudi Chemical Society. 2013;17:53–59.

3. Addel-Gaber AM, Abd-El-Nabey BA, Sidahmed IM, El-Zayady AM, Saadawy M. Kinetics and thermodynamics of aluminium dissolution in 1.0 M sulphuric acid containing chloride ions. Mater. Chem. Phys. 2006;98(2-3):291-297.

4. David EA, Adebiyi A, Gerald I, Edwin O. Corrosion inhibition of mild steel in 0.1M H2SO4 solution by *Anacardium occidentale* Gum. American Chemical Science Journal. 2014;4(6):847-854.

5. Nwosu OF, Osarolube E. Corrosion inhibition of aluminium alloy in 0.75 M KOH alkaline solution using *Xylopia aethiopica* seed extract. Physical Science International Journal. 2014;4(9):1235-1243.

6. Eddy NO. Ethanol extracts of *Phyllanthus amarus* as a green inhibitor for corrosion of mild steel in H2SO4. Portugaliae Electrochemical Acta. 2009;27(5):579-589.

7. Okafor PC, Osabor VI, Ebenso EE. Eco-friendly corrosion inhibitors: Inhibitive action of ethanol extracts of Garcinia Kola for the corrosion of mild steel in H2SO4 solutions. Pigment and Resin Technology. 2007;36:299-305.

8. Umoren SA, Obot IB, Ebenso EE, Okafor PC, Ogbobe O, Oguzie EE. Gum arabic as a potential corrosion inhibitor for aluminum in alkaline medium and its adsorption characteristics. Anti Corrosion Meth Mater. 2006;53:277-282.

9. Nwosu FO, Nnanna LA, Osarolube E. The use of eco-friendly leaf as a corrosion inhibitor of mild steel in an Acidic Environment. Intentional Journal Material Chemistry. 2013;3(3):64-68.

10. Oguzie EE, Oguzie KL, Akalezi, CO, Udeze IO, Ogbulie JN, Njoku VO. Natural products for materials protection: Corrosion and microbial growth inhibition using *Capsicum frutescens* biomass extraction. Chemical Engineering. 2013;1: 214-225.

11. Li XH, Fu H, Deng SD. Inhibition effect of *Dendrocalamus* brandisii leaves extract on steel in hydrochloric acid solution. J Chin Soc Corros Prot. 2011;21:149–54.

12. NIroha NB, Chidiebere MA. Evaluation of the inhibitive effect of *Annona muricata* L. Leaves extract on low carbon steel corrosion in acidic media. International Journal of Materials and Chemistry. 2017; 7(3):47-54.

13. Nwosu FO, Owate IO, Osarolube E. Acidic corrosion inhibition mechanism of auminum alloy uisng green inhibitor. American Journal of Material Science. 2018a;8(3):45-50.

14. Nwosu FO, Owate IO, Osarolube E. Adsorption and corrosion inhibition of *Epiphyllum oxypetalum* leaf extract on aluminum alloy AA5052. Journal of Materials Science Research and Reviews. 2018;1(4):1-11.

15. William DC, David GR. Materials Science and Engineering: An Introduction John Wiley and Sons. Inc. London. 7th Ed; 2007.

16. Sastri VS, Green corrosion inhibitors: Theory and Practice. John Will and Sons Inc; 2011.

17. Shivakumar SS, Mohana KN. Studies on the inhibitive performance of *Cinnamomum zeylanicum* extracts on the corrosion of mild steel in hydrochloric acid and sulphuric acid media. J Mater Environ Sci. 2013;4(3):448-459.

18. Ribeiro DV, Souza CAC, Abrantes JCC, Use of electrochemical impedance spectroscopy (EIS) to monitor the corrosion of reinforced concerte. IBRACON Structures and Materials Journal. 2015;8(4):529-546.

19. Ribeiro DV, Souza CAC, Abrantes JCC. Use of electrochemical impedance spectroscopy (EIS) to monitoring the corrosion of reinforced concrete. Ibracon Structure and Materials Journal. 2015; 8(4):529-546.

20. Morad MS. An electrochemical study on the inhibiting action of some organic phosphonium compounds on the corrosion of mild steel in aerated acid solutions. Corros. Sci. 2000;42:1307-1326.

21. Al-Sabagh AM, Kandil NG, Bdawi AM, El-Sharkawy H. Surface activity and thermodynamic of micellization and adsorption for isooctylphenol ethoxylates, phosphate esters and their mixtures with N-diethoxylated perfluorooctanamide. J. Colloid Surf. A: Physicochem. Eng. Asp. 2000;170:127–136.

22. Aguilar A, Sagüés A, Powers R. Corrosion rates of steel in concrete. ASTM-STP 1065, American Society for Testing and Materials. 1990;66–85.

23. Oguzie EE. Studies on the inhibitive effect of *Occimum virids* extract on the acid corrosion of mild steel. Materials Chemistry and Physics. 2006;99(2-3):441-446.

24. Ashassi-sorkhabi H, Shaabani B, Aligholipour B, Seifzadeh D. The effect of SOE Schiff bases on the corrosion of aluminum in HCl solution. Appl. Surf. Sci. 2006;252:4039-4047.

25. Schockry H, Yuasa M, Sekine I, Issa RM, El-baradie HY, Gomma GK. Corrosion inhibition of mild steel by Schiff base compounds in various aqueous solution. Part I. Corros. Sci. 1998;40:2173–2186.

26. Eddy NO, Ita BI. QSAR, DFT and quantum chemical studies on the inhibition potential of some carbozones for the corrosion of mild steel in HCl. Journal of Molecular Modeling. 2010;17(2):239-363.

27. Ebenso EE. Synergistic effect of halide ions on the corrosion inhibition of aluminium in H_2SO_4 using 2-acetyl-phenothiazine. Mater. Chem and Phys. 2003;79:58-70.

28. Matai S, Bagchi DK, In A. Granam SI. Krishaswamy JS, Kaha, (eds). Proceedings international symposium on biological applications of solar energy. Mandras: Macmillan Company of India. 1980;144-148.

29. Noor EA, Al-Moubaraki AH. Thermo-dynamics of metal corrosion and inhibition adsorption process in mild steel/1-methyl-4[4′(-X)-styrylpyridiniumiodides/

hydrochloric acid systems. Journal of Material Chemistry and Physics. 2008;110: 145-154.

30. Bhajiwala HM, Vashi RT. Ethanolamine, diethanolamine and triethanolamine as corrosion inhibitors for zinc in binary acid mixture ($HNO_3 + H_3PO_4$). Bull. Electochem, 2001;17:411–448.

31. Zerga B, Attayibat A, Sfaira M, Taleb M, Hammouti B, Ebn Touhami M, Radi S, Rais Z. Effect of some tripodal bipyrazolic compounds on C38 steel corrosion in hydrochloric acid solution. Journal of Applied Electrochemistry. 2010; 40:1575.
Available:https://doi.org/10.1007/s10800-010-0164-0

32. Awe C, Abdulrahaman AS, Ibrahim HK, Kareem AG, Adams SM. Inhibitive performance of bitter leaf root extract on mild steel corrosion in sulphuric acid solution. American Journal of Materials Engineering and Technology. 2015;3(2): 35-45.

33. Prathibha BS, Kotteeswaran P, Raju VB. Study on the inhibition of mild steel corrosion by N, N-dimethyl-N-(2-phenoxyethyl)dodecan-1-aminiumbromide in HCl mediun. IOSR Journal of Applied Chemistry. 2013;5(1):1-10.

34. Aqida SN, Ghazali MI, Hashim J. Effects of porosity on mechanical properties of metal matrix composite: An overview. Jurnal Teknologi. 2004;40(A):17–32.